



Lattice Boltzmann schemes for the *Brinkman equation* in extremely heterogeneous porous media: bulk, boundary, interface

Gonçalo Silva & Irina Ginzburg

Groupe de travail “Schémas de Boltzmann sur réseau”

6th May 2015

1 Who am I?

- PhD work
- Experiments
- Numerics

2 Context

- Motivation

3 TRT-LBM

- Properties

4 Channels

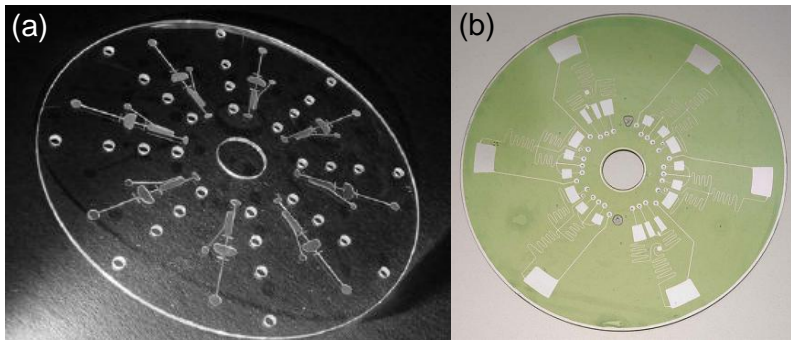
- Bulk
- Boundary/interface
- Boundary/interface
- Solutions
- Conclusions

5 Non-channels

- Benchmark description

- Approximated solutions
- Stokes flow around solid cylinder
- Porous flow around solid cylinder
- Conclusions
- Biporous medium: Introduction
- Porous flow across porous cylinder $k_1 \ll k_2$
- Porous flow across porous cylinder $k_1 \gg k_2$
- Conclusions

Theoretical, numerical and experimental characterization of microfluidic channel flows in rotating platforms

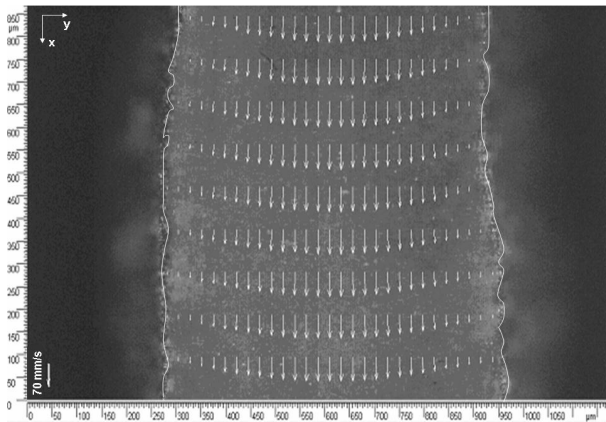


Examples of lab-on-a-CD prototypes, (a) *image source*: Brenner *et al.* 2003; (b) *image source*:

www.spaceref.com

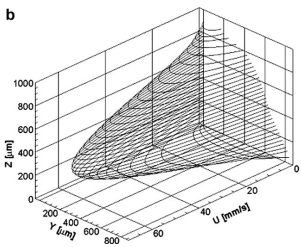
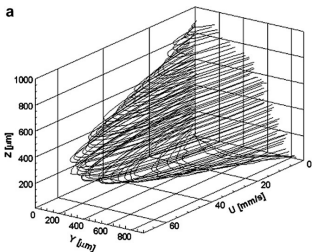
Experiments

Example of micro-PIV measurement

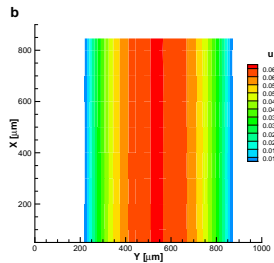
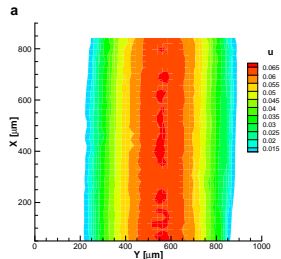


Experiments

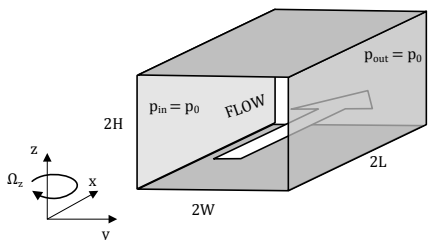
Micro-PIV



CFD

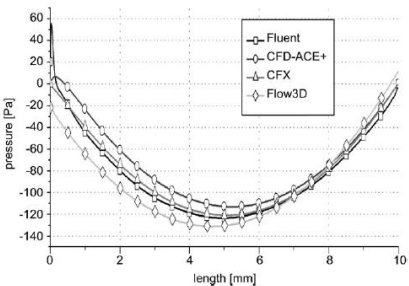


A simple numerical verification test



Centrifugal-driven rotating channel

flow setup



Streamwise pressure solution predicted by several commercial CFD codes

– image source: Glatzela et al. 2008

Numerics

LBM studies:

Blends A 300 (2011) 1085–1096



A study on the inclusion of body forces in the lattice Boltzmann BGK equation to recover steady-state hydrodynamics

Goncalo Silva, Viriato Semiao*

Manoel Freitas-silva, Francisco-José Serrano-Torres, Faculty of Sciences and Technology, University of Lisbon, Av. das Forças Armadas, 1649-026 Lisboa, Portugal.

J. Fluid Mech., page 1 of 22. © Cambridge University Press 2012
doi:10.1017/jfm.2012.83

1

First- and second-order forcing expansions in a lattice Boltzmann method reproducing isothermal hydrodynamics in artificial compressibility form

Goncalo Silva and Viriato Semiao[†]

TU Lisbon, Instituto Superior Técnico, IDMEC, Department of Mechanical Engineering, P-1049001
Lisbon, Portugal

(Received 6 October 2011; revised 22 December 2011; accepted 7 February 2012)

Journal of Computational Physics 269 (2014) 259–271



Truncation errors and the rotational invariance of three-dimensional lattice models in the lattice Boltzmann method



Goncalo Silva^{*}; Viriato Semiao

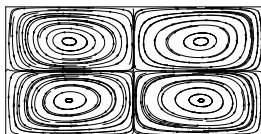
University of Lisbon, Instituto Superior Técnico, IDMEC - Department of Mechanical Engineering, P-1049001 Lisbon, Portugal

Numerics

Results: $Ek^{-1} \equiv \frac{\Omega_z H^2}{\nu} = 0.001$

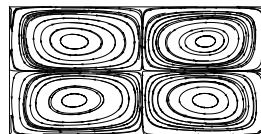
(a)

D3Q15



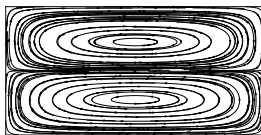
(b)

D3Q19



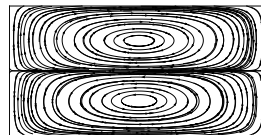
(c)

D3Q27



(d)

ACM

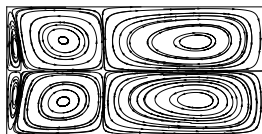


Numerics

Results: $Ek^{-1} \equiv \frac{\Omega_z H^2}{\nu} = 0.02$

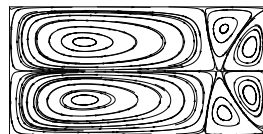
(a)

D3Q15



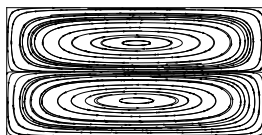
(b)

D3Q19



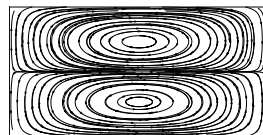
(c)

D3Q27



(d)

ACM

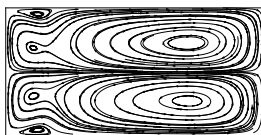


Numerics

Results: $Ek^{-1} \equiv \frac{\Omega_z H^2}{\nu} = 0.05$

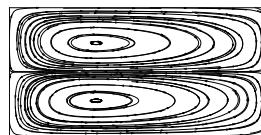
(a)

D3Q15



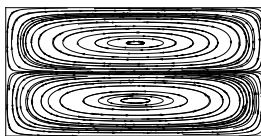
(b)

D3Q19



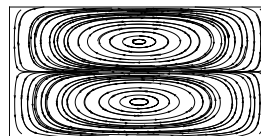
(c)

D3Q27



(d)

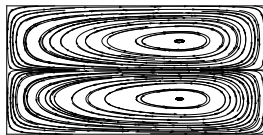
ACM



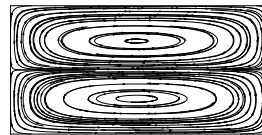
Numerics

Results: $Ek^{-1} \equiv \frac{\Omega_z H^2}{\nu} = 0.1$

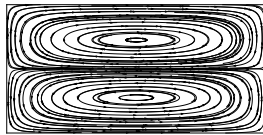
(a) D3Q15



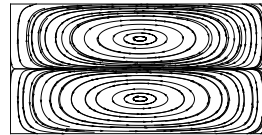
(b) D3Q19



(c)



(d) **ACM**

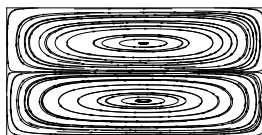


Numerics

Results: $Ek^{-1} \equiv \frac{\Omega_z H^2}{\nu} = 1$

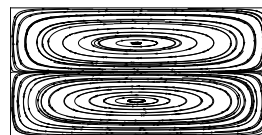
(a)

D3Q15



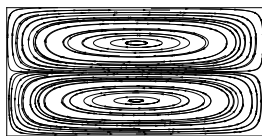
(b)

D3Q19



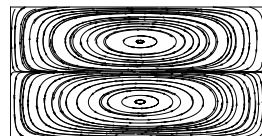
(c)

D3Q27



(d)

ACM



Motivation

Heterogeneous porous media systems

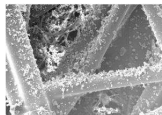


Figure 1: SEM [Scanning Electron Microscope] view of used cabin automotive air filter

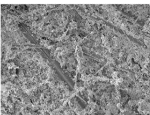


Figure 3: SEM of dust loaded filter has passed the depth filtration stage (transition stage)

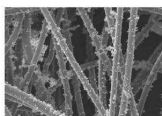


Figure 2: SEM representing the stationary stage of dust loading

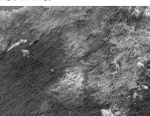


Figure 4: SEM of dust cake formation on the filter surface

image source: www.ntu.edu.sg

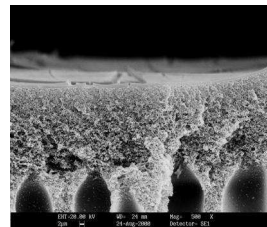


image source: www.memfil.com

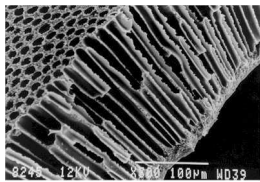
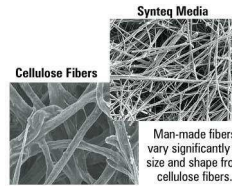


image source: www.ntu.edu.sg



Man-made fibers vary significantly in size and shape from cellulose fibers.

Figure 2. Liquid Filtration Media

Motivation

 Governing equations
(nondimensional)

Stokes-Brinkman-Darcy equations

$$\vec{\nabla} \cdot \vec{u} = 0$$

$$f(\phi) \vec{\nabla} p = \Delta \vec{u} - \sigma^2 \vec{u}$$

subject to proper interface/solid BC.

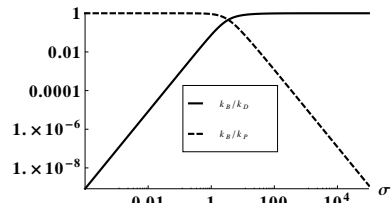
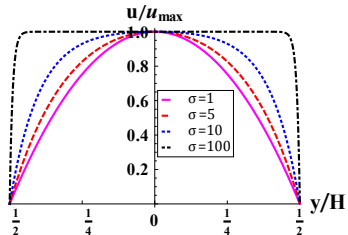
Solution is controlled by:

- $f(\phi)$ (herein = 1, for simplicity)
- $\sigma^2 = f(\phi) H^2/k$

Given $\sigma \Rightarrow 3$ dynamical regimes follow:

- ① $\sigma < 1$: “Open” flow \rightarrow Stokes
- ② $\sigma \sim 1$: “Interface” flow \rightarrow Brinkman
- ③ $\sigma > 1$: “Constant” flow \rightarrow Darcy

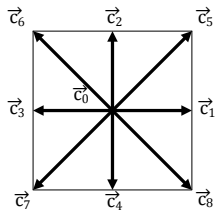
Channel flow solutions:



Properties

D2Q9

LB evolution equation:



① Streaming: $f_q(\vec{r} + \vec{c}_q, t + 1) = \tilde{f}_q(\vec{r}, t)$

② TRT collision:

$$\tilde{f}_q(\vec{r}, t) = f_q(\vec{r}, t) + g_q^+ + g_q^-$$

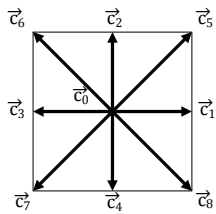
where $g_q^\pm = -s^\pm (f_q^\pm - e_q^\pm)$ defined by:

- Symmetric equilibrium $e_q^+ = t_q P(\rho)$
- Anti-symmetric equilibrium $e_q^- = j_q + \Lambda^- F_q$
with $j_q = t_q (\vec{j} \cdot \vec{c}_q)$ and $F_q = t_q (\vec{F} \cdot \vec{c}_q)$
- Relaxation functions $\Lambda^\pm = \left(\frac{1}{s^\pm} - \frac{1}{2} \right) > 0$
with $s^\pm \in]0, 2[$
- Brinkman viscosity $\nu_B = \frac{\nu}{f(\phi)} = \frac{\Lambda^+}{3}$

Properties

D2Q9

LB evolution equation:



③ Conservation:

- Mass $\rho = \sum_{q=0}^{Q-1} f_q$
- Momentum $\rho_0 \vec{u} = \vec{j} = \sum_{q=1}^{Q-1} \vec{c}_q f_q - \frac{1}{2} \vec{F}$

④ Invariance:

- Steady-state solutions are fixed by $\Lambda = \Lambda^+ \Lambda^-$ (viscosity-independence)

⑤ BF scheme:

- Brinkman force term: $\vec{F} = \vec{F}^p - B_f \vec{j}$ with $B_f = \frac{\nu}{k}$

⑥ IBF scheme:

- Introduce redefine symmetric relaxation function, e.g. $\Lambda_*^+ = \frac{3(4+B)\Lambda^+}{4(3+2B\Lambda)}$ where $B = \frac{\sigma^2}{H^2}$ or $B = \frac{B_f}{\nu_B}$

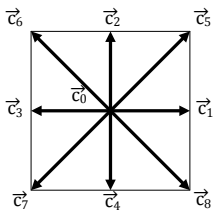
Properties

Steady-state recurrence equations:

- ➊ One pair of linear combinations per link:

$$g_q^+ = \bar{\Delta}_q e_q^- - \Lambda^- \bar{\Delta}_q^2 e_q^+ + \left(\Lambda - \frac{1}{4}\right) \bar{\Delta}_q^2 g_q^+$$

$$g_q^- = \bar{\Delta}_q e_q^+ - \Lambda^+ \bar{\Delta}_q^2 e_q^- + \left(\Lambda - \frac{1}{4}\right) \bar{\Delta}_q^2 g_q^-$$



- ➋ And another pair per link:

$$\bar{\Delta}_q g_q^- = \bar{\Delta}_q^2 e_q^+ - \Lambda^+ \bar{\Delta}_q^2 g_q^+$$

$$\bar{\Delta}_q g_q^+ = \bar{\Delta}_q^2 e_q^- - \Lambda^- \bar{\Delta}_q^2 g_q^-$$

where first and second central linkwise finite differences are:

- $\bar{\Delta}_q \psi = \frac{1}{2} (\psi(\vec{r} + \vec{c}_q) - \psi(\vec{r} - \vec{c}_q))$
- $\bar{\Delta}_q^2 \psi = \psi(\vec{r} + \vec{c}_q) - 2\psi(\vec{r}) + \psi(\vec{r} - \vec{c}_q)$

General solution:

- Exact steady macroscopic equations:

$$\sum_{q=0}^{Q-1} g_q^+ = 0, \quad \sum_{q=1}^{Q-1} g_q^- \vec{c}_q = \vec{F}$$

- Taking the moments of recurrence equations g_q^\pm :

$$① \quad \bar{\nabla} \cdot \vec{j} = \Lambda^- \bar{\Delta}^2 P - \left(\Lambda - \frac{1}{4} \right) \sum_{q=1}^{Q-1} \bar{\Delta}_q^2 g_q^+$$

$$② \quad \bar{\nabla} P - \vec{F} = \frac{\Lambda^+}{3} \bar{\Delta}^2 \vec{j} + \Lambda \sum_{q=1}^{Q-1} \bar{\Delta}_q^2 F_q^- \vec{c}_q - \left(\Lambda - \frac{1}{4} \right) \sum_{q=1}^{Q-1} \bar{\Delta}_q^2 g_q^- \vec{c}_q$$

- $\bar{\nabla} \cdot \vec{j} = \sum_{q=1}^{Q-1} \bar{\Delta}_q j_q$
- $\bar{\Delta}^2 P = \sum_{q=1}^{Q-1} \bar{\Delta}_q^2 P_q$
- $\bar{\nabla} P = \sum_{q=1}^{Q-1} \bar{\Delta}_q P_q \vec{c}_q$
- $\bar{\Delta}^2 \vec{j} = 3 \sum_{q=1}^{Q-1} \bar{\Delta}_q^2 j_q \vec{c}_q$

- Isotropic correction
(Brinkman eq.):
 $\Lambda \sum_{q=1}^{Q-1} \bar{\Delta}_q^2 F_q^- \vec{c}_q = -\frac{\Lambda B_f}{3} \bar{\Delta}^2 \vec{j}$
- Anisotropic correction
(Brinkman eq.):
 $\left(\Lambda - \frac{1}{4} \right) \sum_{q=1}^{Q-1} \bar{\Delta}_q^2 g_q^- \vec{c}_q = ?$

Channel solution:

Straight/diagonal channel in rotated coordinate system (x', y') :

- ① Momentum: $\sum_{q=1}^{Q-1} g_q^- c_{qx'} = F_{x'}$ $\implies g_q^- = 3t_q F_{x'}(y') c_{qx'} c_{qy'}^2$
- ② Periodic condition: $g_q^- = 0$ if $c_{qy'} = 0$

Anisotropic correction (Brinkman eq.):

$$\left(\Lambda - \frac{1}{4}\right) \sum_{q=1}^{Q-1} \bar{\Delta}_q^2 g_q^- \vec{c}_q = -3 \left(\Lambda - \frac{1}{4}\right) B_f \bar{\Delta}_{y'}^2 j_{x'} \sum_{q=1}^{Q-1} t_q c_{qx'}^2 c_{qy'}^2 = \\ -\left(\Lambda - \frac{1}{4}\right) B_f \bar{\Delta}_{y'}^2 j_{x'}$$

Total correction (Isotropic+Anisotropic):

$$-\frac{\Lambda B_f}{3} \bar{\Delta}_{y'}^2 j_{x'} + \left(\Lambda - \frac{1}{4}\right) B_f \bar{\Delta}_{y'}^2 j_{x'} = B_f \left(\frac{8\Lambda-3}{12}\right) \bar{\Delta}_{y'}^2 j_{x'}$$

Channel solution:

Brinkman forcing modifies effective viscosity of Laplacian term

$$\bar{\nabla}_{x'} P - F_{x'} = \frac{\Lambda^+}{3} \rho_0 (1 + \delta) \bar{\Delta}_{y'}^2 u_{x'}$$

$$\text{where } \delta = B \left(\frac{8\Lambda - 3}{12} \right) \text{ with } B = \frac{3B_f}{\Lambda^+}$$

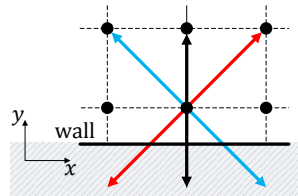
Observations:

- Consistency requires viscosity independent solutions.
Impossible for BGK since $\Lambda = (\tau - \frac{1}{2})^2$ makes $\delta(B, \nu) \neq 0$!
- No numerical oscillations require $\delta > -1$,
straight channel: $B < \frac{12}{3-8\Lambda}$.
- Idea of IBF, giving $\Lambda^+ = 3\nu_B$, $B_f = \nu/k$ and Λ , redefine:
 $\Lambda^+ \rightarrow \Lambda_*^+ (\nu_B, B_f, \Lambda)$. Example, $\Lambda_*^+ = \frac{9(4+B)\nu_B}{4(3+2B\Lambda)}$ makes $\delta = 0$.

Boundary/interface

Solid wall:

- **Bounce-back:** $f_q(\vec{r}_b, t + 1) = \tilde{f}_{\bar{q}}(\vec{r}_b, t)$
with $\vec{c}_{\bar{q}} = -\vec{c}_q$ and $\vec{r}_b + \vec{c}_q \in \text{solid}$



For a straight channel of width H , the bounce-back closure relation reads:

$$u_x \pm \frac{1}{2} \alpha^+ \bar{\Delta}_y u_x + \frac{1}{8} \alpha^- \bar{\Delta}_y^2 u_x \Big|_{y_{\text{wall}}=\pm \frac{H}{2} \mp \frac{1}{2}} = 0$$

with $\alpha^+ = (1 + \delta)$ and $\alpha^- = (1 + \delta) \frac{16}{3} \Lambda$
(different coefficient values for IBF)

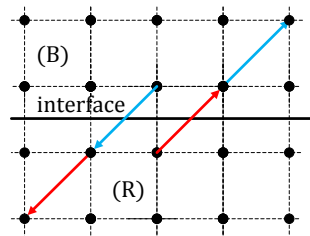
Boundary/interface

Interface:

• Implicit interface

$$\begin{cases} f_q(\vec{r}^{(B)}, t+1) = \tilde{f}_q(\vec{r}^{(R)}, t) \\ \tilde{f}_{\bar{q}}(\vec{r}^{(B)}, t) = f_{\bar{q}}(\vec{r}^{(R)}, t+1) \end{cases}$$

$$\text{with } \vec{r}^{(B)} = \vec{r}^{(R)} + \vec{c}_q$$



For stratified channels the steady-state closure relation for the (implicit) interface reads:

$$\|\nu_i (\bar{\Delta}_y u_x^{(i)} \pm \frac{1}{2} \bar{\Delta}_y^2 u_x^{(i)})\|_{Y_i \mp \frac{H}{2}} = 0, \quad \nu_i = \nu_B^{(i)} (1 + \delta_i),$$

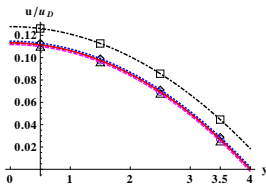
$$\|u_x^{(i)} \pm \frac{1}{2} \alpha^+ \bar{\Delta}_y u_x^{(i)} + \frac{1}{8} \alpha^- \bar{\Delta}_y^2 u_x^{(i)}\|_{Y_i \mp \frac{H}{2}} = 0$$

with $\alpha^+ = (1 + \delta)$ and $\alpha^- = (1 + \delta) \frac{16}{3} \Lambda$
(different coefficient values for IBF)

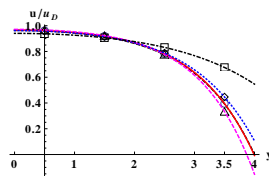
Solutions

Bounded channel

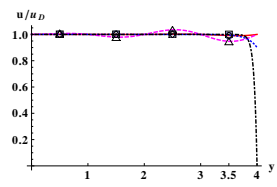
Solutions width $H = 8$ with $\Lambda = \{\frac{1}{512}, \frac{3}{16}, \frac{3}{8}, 2\}$



Stokes-Brinkman regime
($\sigma = 1$)



Brinkman regime ($\sigma = 8$)



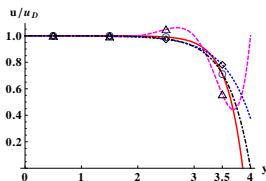
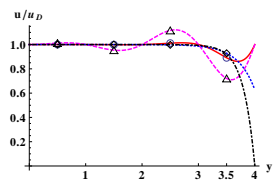
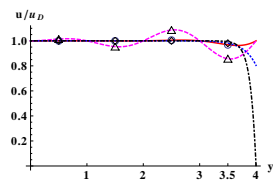
Darcy-Brinkman regime
($\sigma = 160$)

Solutions

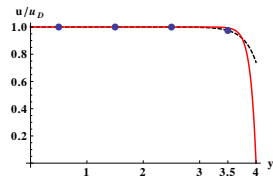
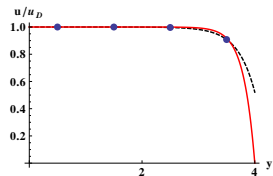
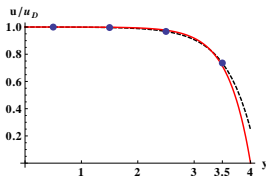
Bounded channel

Solutions width $H = 8$ with $\Lambda = \left\{ \frac{1}{512}, \frac{3}{16}, \frac{3}{8} \right\}$

BF:

Brinkman regime ($\sigma = 20$)Brinkman regime ($\sigma = 40$)Brinkman regime ($\sigma = 80$)

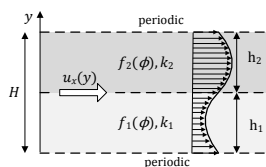
IDF:



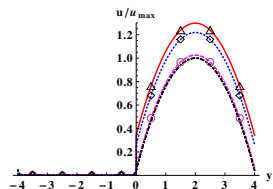
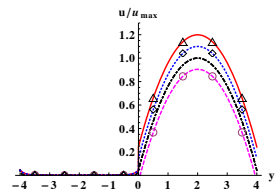
Solutions

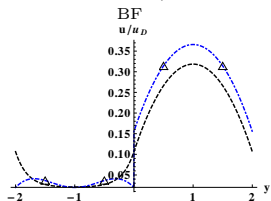
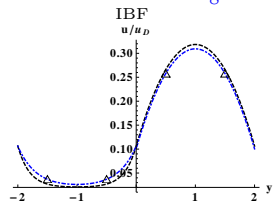
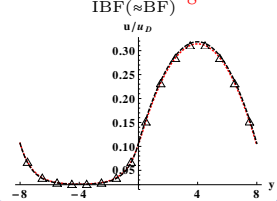
Unbounded channel

Solutions width $H = 8$ with $\Lambda = \{\frac{1}{512}, \frac{1}{8}, \frac{3}{16}\}$



Periodic unbounded channel

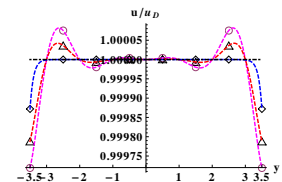
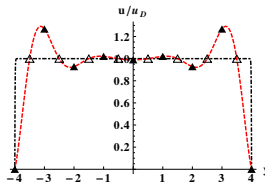
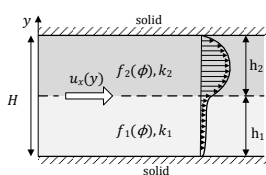

 $\sigma \approx 0.26, k_2/k_1 = 10^6$ (BF)

 $\sigma \approx 0.26, k_2/k_1 = 10^6$ (IBF)

 $\sigma \approx 2.8, k_2/k_1 = 10^2$:

 $H = 4$ and $\Lambda = \frac{1}{8}$

 $H = 8$ and $\Lambda = \frac{1}{8}$
IBF(\approx BF)


Solutions

Bounded layered channel: FEM vs TRT (BF)

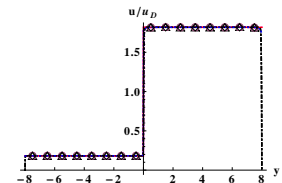
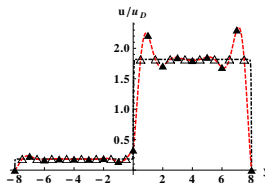
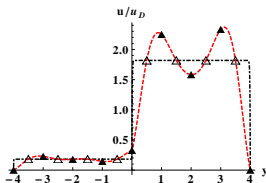
Solutions width $H = 8$ with $\Lambda = \left\{ \frac{1}{512}, \frac{3}{16}, \frac{3}{8} \right\}$



Bounded stratified channel

 $\sigma = 10^3, k_2 = k_1$ (FEM/BF)

 $\sigma = 10^3, k_2 = k_1$ (BF)

 $H = \{8, 16\}$ and $\Lambda = \left\{ \frac{1}{8} \right\}$
 $\sigma = 10^3, k_2/k_1 = 10$ $H = 16$ and $\Lambda = \left\{ \frac{1}{8}, \frac{3}{16}, \frac{3}{8} \right\}$


Conclusions

Brinkman flow in bounded channels: boundary condition

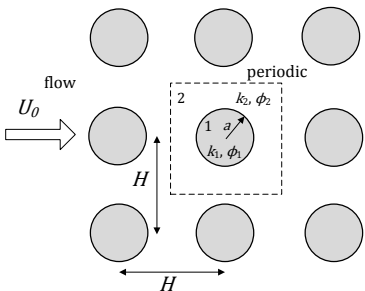
- Physical solution experiences three regimes: Stokes, Brinkman, Darcy.
- Discrete solution is controlled by bulk and boundary approximations.
- Bulk error in BF is vanished for $\Lambda = 3/8$. For $\Lambda < 3/8$ may lead to wiggles in bulk solution. Bulk error is absent by construction in IBF.
- Bounce-back boundary error is always present (already at the 1st order) for $B \neq 0$ (when $B = 0$, it is exact for $\Lambda < 3/16$).
- Bounce-back prescribes boundary implicitly. It allows smoother bulk accommodation on wall. Enforcement on wall nodes triggers oscillations, e.g. FEM.

Brinkman flow in layered channels: interface condition

- Discrete solution is controlled by bulk and interface approximations.
- Implicit interface prescription may lead to jumps in continuity conditions.
- Interface continuity is only exact for $B = 0$ (Stokes). Interface jumps increase for $B \gg 1$ (Darcy). They decrease for $\Lambda \ll 1$, but produce wiggles. Solution: IBF.

Benchmark description

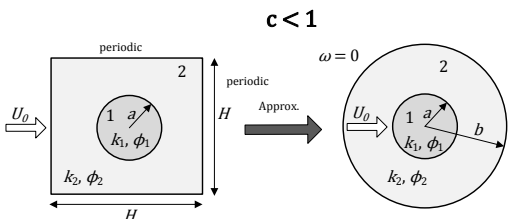
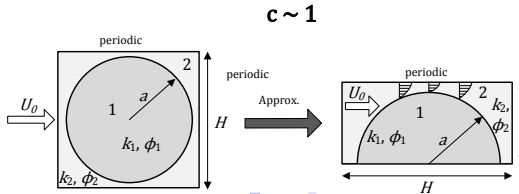
Idealized geometry:



Characteristic parameters:

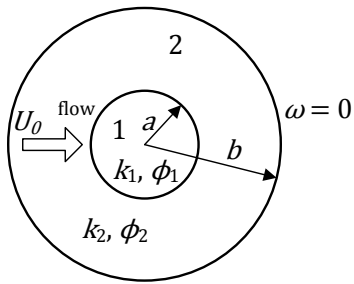
- Obstacles configuration:
Square array arrangement
- Obstacles concentration:

$$c = \frac{\pi a^2}{H^2}$$

Cell model
(dilute limit):Lubrication theory
(high concentration limit):

Approximated solutions

Cell model:



Main features:

- Ratio of particle to cell volume c remains invariant
- Independent of packing arrangement (in principle requires $c \ll 1$)
- Approximation on outer BC:
 $\omega = 0$ (Kuwabara model)
- Polar coordinates:
 $(x, y) \mapsto (r, \theta)$
- Streamfunction formulation:
 $u_r = \frac{1}{r} \frac{\partial \psi}{\partial \theta}$ and $u_\theta = -\frac{\partial \psi}{\partial r}$

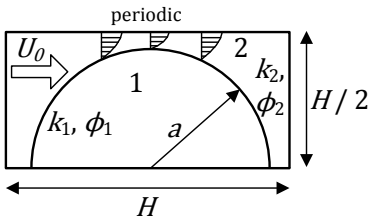
General solution (Brinkman):

$$\psi^{(i)}(r, \theta) = \left(\frac{C_1^{(i)}}{r} + C_2^{(i)}r + C_3^{(i)}I_1(\sigma_1 r) + C_4^{(i)}K_1(\sigma_1 r) \right) \sin(\theta)$$

subject to proper interface/solid BC

Approximated solutions

Lubrication theory:



General solution (Brinkman):

$$u_x^{(i)}(y) = -\frac{1}{\sigma_i^2} \frac{dp}{dx} + C_1^{(i)} \exp(y\sigma_i) + C_2^{(i)} \exp(-y\sigma_i)$$

subject to proper interface/solid BC

Main features:

- Ratio of particle to cell volume c remains invariant
 - Depends on packing arrangement
 - Approximation in bulk: flow asymptotically unidirectional (Lubrication model)
 - Caution: singular behaviour when $H/2 - a \rightarrow 0$

Approximated solutions

Permeability computations:

Cell model

$$F = \int_0^{2\pi} \left((-p^{(2)} + \tau_{rr}^{(2)}) \cos(\theta) - \tau_{r\theta}^{(2)} \sin(\theta) \right)_{r=b} b \, d\theta$$

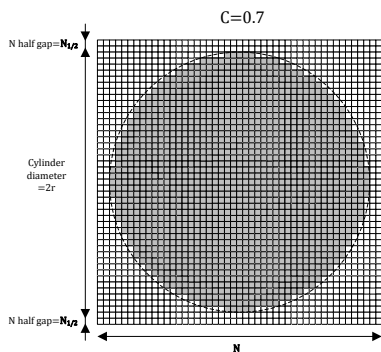
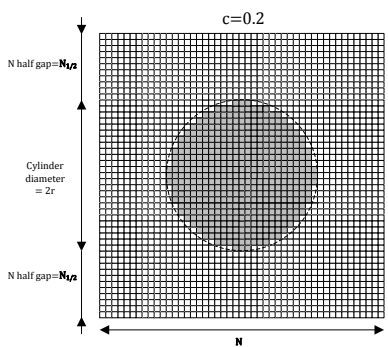
$$k_{eff} = \frac{U_0}{F/V} = \frac{U_0 \pi b^2}{F}$$

Lubrication theory

$$Q = \int_0^{a(x)} u_x^{(1)} \, dy + \int_{a(x)}^{H/2} u_x^{(2)} \, dy = \frac{-f(x)}{\mu} \frac{dp}{dx}$$

$$k_{eff} = \frac{4a}{H} \left(\int_0^a \frac{1}{f(x)} \, dx \right)^{-1}$$

Domain discretization

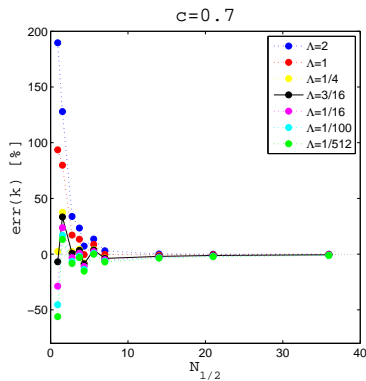
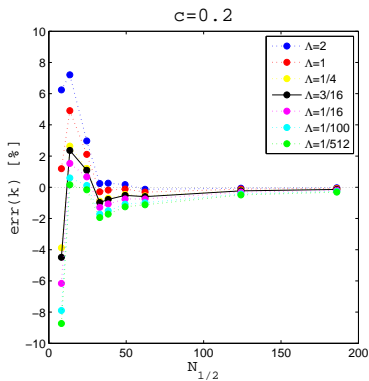


Solid cylinder is discretized in a regular grid by *bounce-back* (i.e. as staircase shape), introducing a discretization error of $O(N^{-1})$

Note: Numerical solutions are evaluated for one half gap size – $\underline{N_{1/2}}$

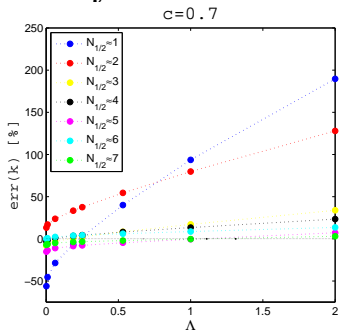
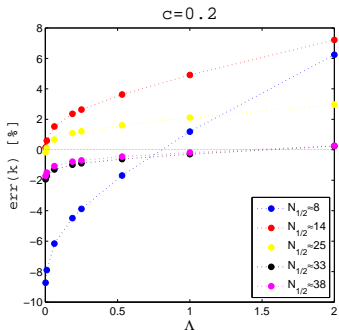
Stokes flow around solid cylinder

Effect of lattice resolution on accuracy



is non-monotonic and with large dependency on Λ at coarse resolutions

Stokes flow around solid cylinder

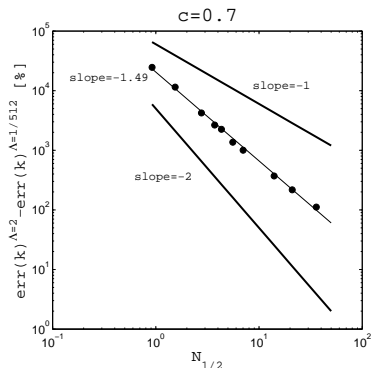
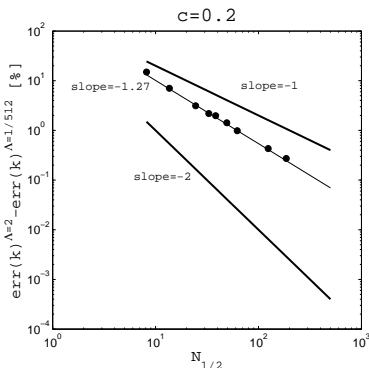
Effect of Λ on accuracy

For fixed lattice resolution Λ controls Stokes solution accuracy through the location of *bounce-back* solid boundary

Remarks:

- ① Staircase representation of cylinder reduces its true hydraulic diameter \Rightarrow makes permeability solution converge to a smaller value
- ② Large Λ reduces hydraulic diameter of cylinder \Rightarrow under-estimates permeability at fixed grid resolution, i.e. $\frac{\partial \text{err}(k)}{\partial \Lambda}|_N > 0$

Effect of lattice resolution on accuracy



becomes monotonic taking difference between any two Λ solutions

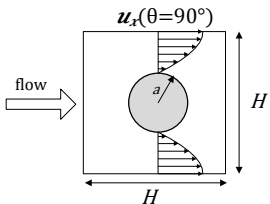
- Spatial convergence rate is between 1st- and 2nd-order

Porous flow around solid cylinder

Stokes regime

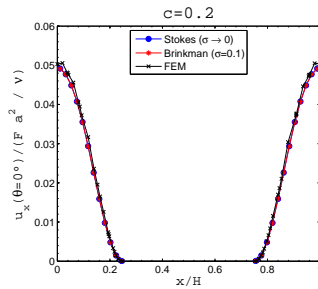
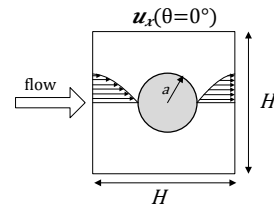
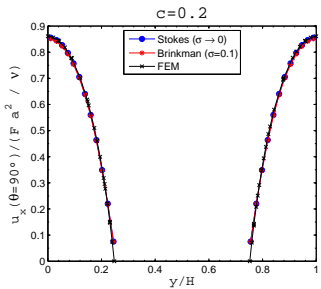
\iff

$$\vec{\nabla} p = \Delta \vec{u} - \underbrace{\sigma^2 \vec{u}}_{\sigma \rightarrow 0}$$



$$u_x(\theta=90^\circ)$$

$$u_x(\theta=0^\circ)$$

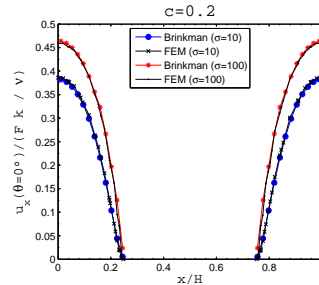
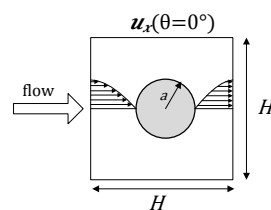
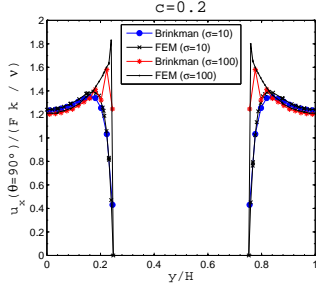
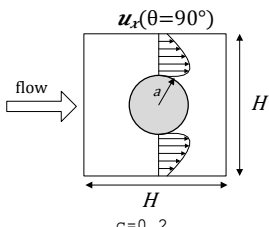


Porous flow around solid cylinder

Brinkman regime

 \iff

$$\vec{\nabla}p = \Delta\vec{u} - \underbrace{\sigma^2\vec{u}}_{\sigma \sim O(1)}$$

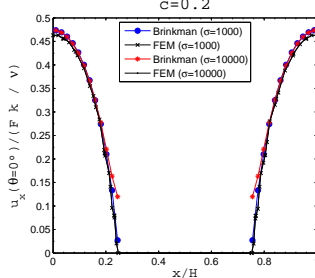
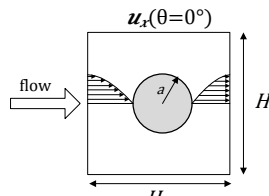
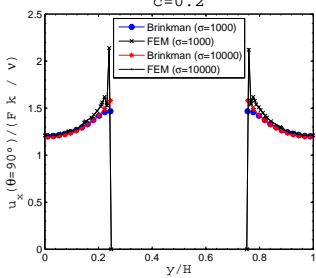
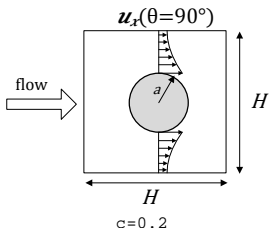


Porous flow around solid cylinder

Darcy regime

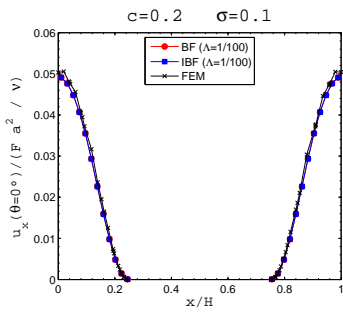
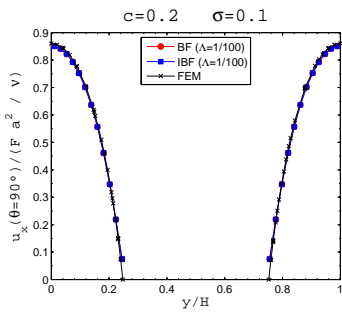
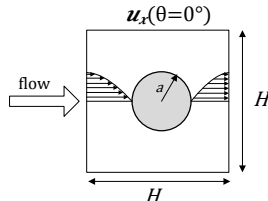
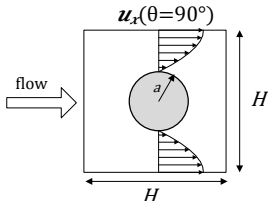
 \iff

$$\vec{\nabla} p = \Delta \vec{u} - \underbrace{\sigma^2 \vec{u}}_{\sigma \rightarrow \infty}$$



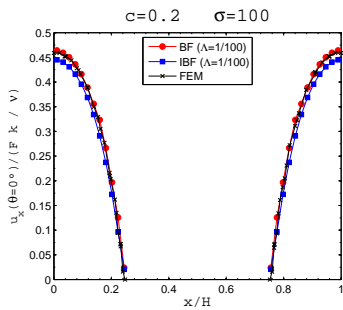
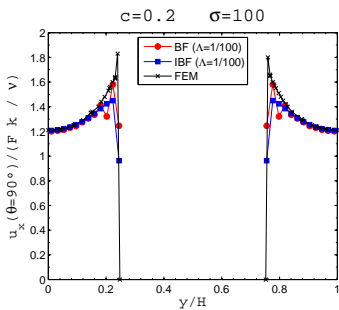
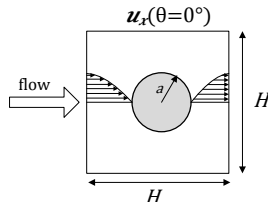
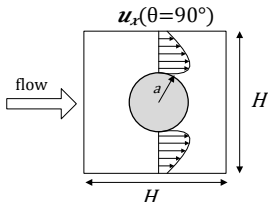
Porous flow around solid cylinder

Stokes regime (with IBF)



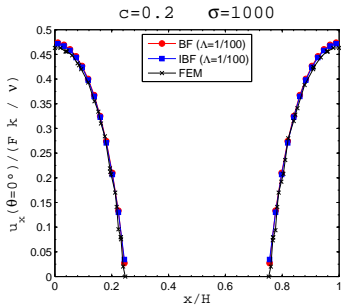
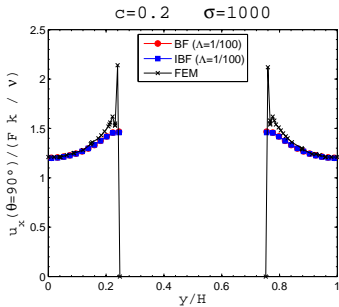
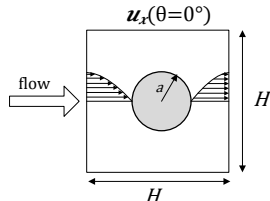
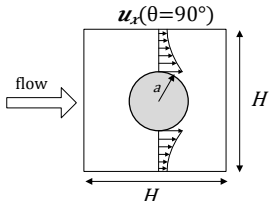
Porous flow around solid cylinder

Brinkman regime (with IBF)



Porous flow around solid cylinder

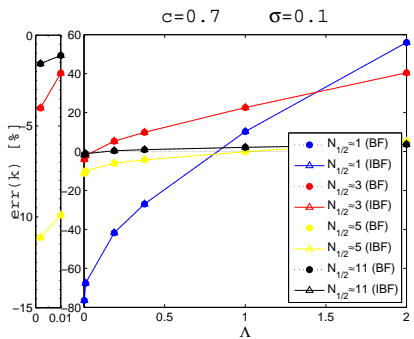
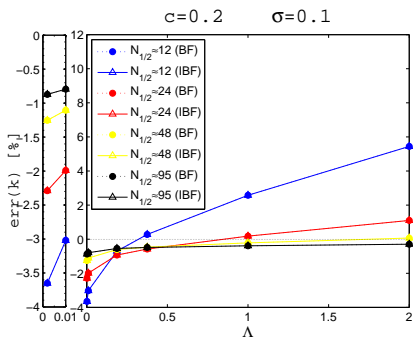
Darcy regime (with IBF)



Porous flow around solid cylinder

Effect of Λ on accuracy

Stokes regime

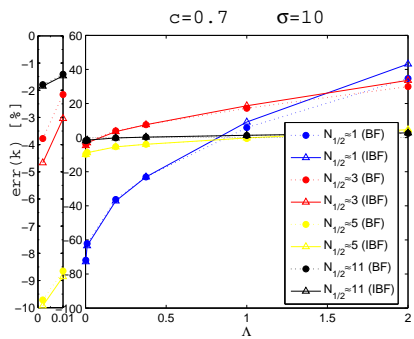
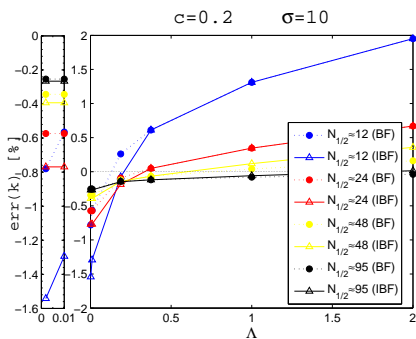


Essentially similar to TRT Stokes solver $\Rightarrow \Lambda$ controls the accuracy through the location of *bounce-back* solid boundary

Porous flow around solid cylinder

Effect of Λ on accuracy

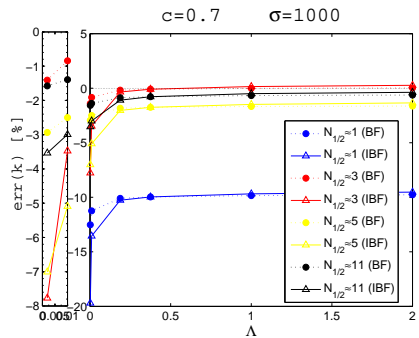
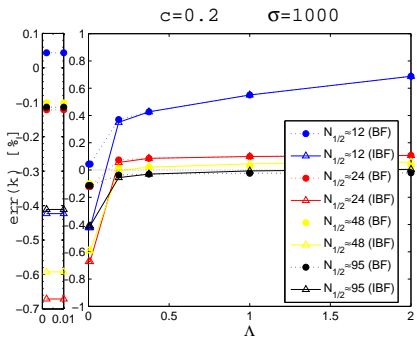
Brinkman regime



Brinkman correction (in bulk and boundary) now plays a role
 \Rightarrow smaller influence of Λ over accuracy (compared to Stokes)

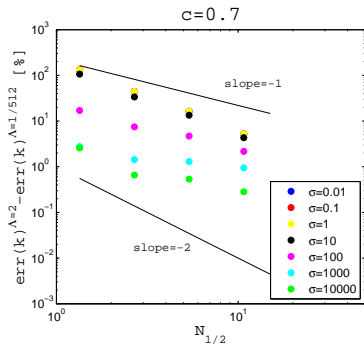
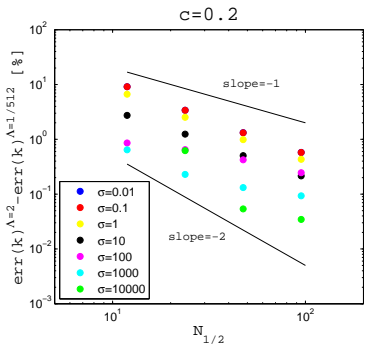
Effect of Λ on accuracy

Darcy regime



Accuracy becomes independent of Λ
except at small Λ values

Effect of lattice resolution on accuracy



$\forall \sigma$ spatial convergence rate between 1st- and 2nd-order
 (Data shown for BF model)

Conclusions

Stokes flow around solid cylinder

- Role of Λ controls the location of the bounce-back solid boundary (by varying the size of cylinder)
- Dependency on Λ is larger at coarser lattice resolutions
- Dependency on lattice resolution indicates spatial convergence rate between 1st – and 2nd–order

Porous flow around solid cylinder

- 3 physical regimes: Stokes $\sigma \ll 1$, Brinkman $\sigma \sim O(1)$, Darcy $\sigma \gg 1$
- Stokes regime: role of Λ controls the location of the bounce-back solid boundary \Rightarrow accuracy is worst and larger dependency on Λ
- Brinkman regime: role of Λ controls both bulk and boundaries errors (Brinkman correction). Better accuracy for k . Yet, velocity solutions may experience wiggles \Leftarrow IBF corrects them ☺
- Darcy regime: role of Λ tends to cease, except at small Λ values
- Effect of lattice resolution indicates spatial convergence rate between 1st – and 2nd–order $\forall \sigma$ regimes

Biporous medium: Introduction

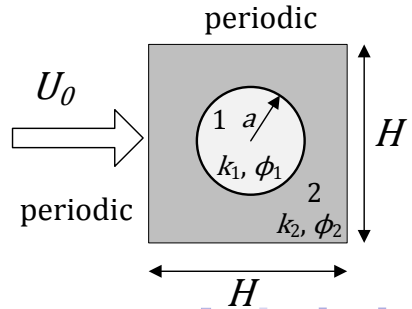
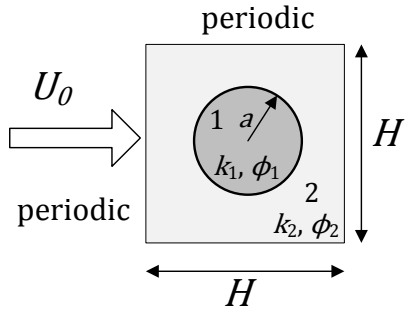
Two physical problems to distinguish from:

1) Porous cylinder is less permeable than outside porous medium

$$\frac{k_1}{k_2} < 1$$

2) Porous cylinder is more permeable than outside porous medium

$$\frac{k_1}{k_2} > 1$$

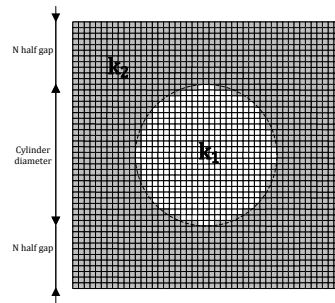
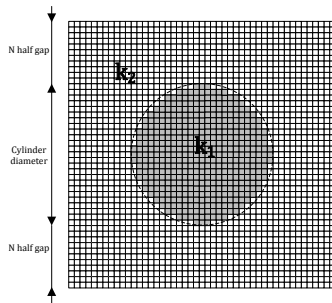


Biporous medium: Introduction

In both cases, **interface** continuity conditions are set *implicitly* and approximate a *staircase* cylinder

$$\frac{k_1}{k_2} < 1$$

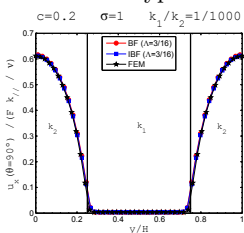
$$\frac{k_1}{k_2} > 1$$



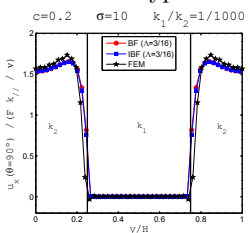
Porous flow across porous cylinder $k_1 \ll k_2$

$u_x(y)$ at vertical ($\theta = 90^\circ$) midplane for $\frac{k_1}{k_2} = \frac{1}{1000}$ and $c = 0.2$

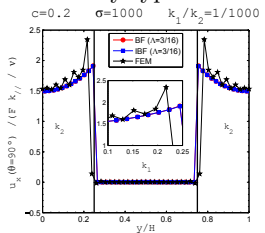
“Stokes-type flow”



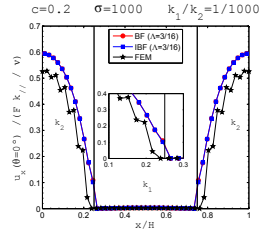
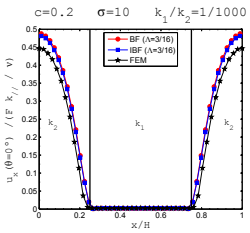
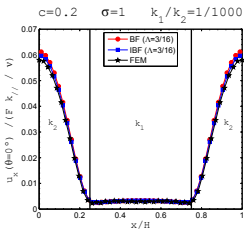
“Brinkman-type flow”



“Darcy-type flow”



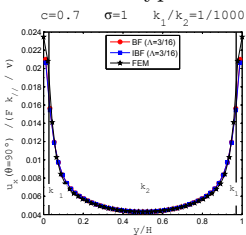
$u_x(x)$ at horizontal ($\theta = 0^\circ$) midplane for $\frac{k_1}{k_2} = \frac{1}{1000}$ and $c = 0.2$



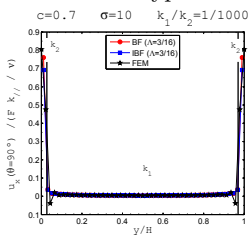
Porous flow across porous cylinder $k_1 \ll k_2$

$u_x(y)$ at vertical ($\theta = 90^\circ$) midplane for $\frac{k_1}{k_2} = \frac{1}{1000}$ and $c = 0.7$

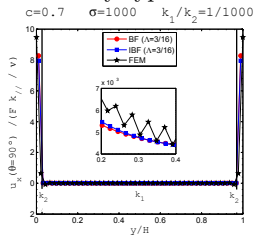
“Stokes-type flow”



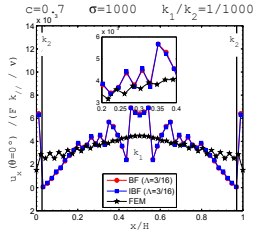
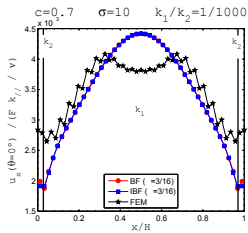
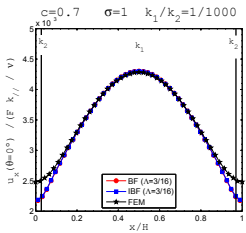
“Brinkman-type flow”



“Darcy-type flow”



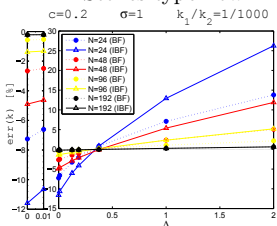
$u_x(x)$ at horizontal ($\theta = 0^\circ$) midplane for $\frac{k_1}{k_2} = \frac{1}{1000}$ and $c = 0.7$



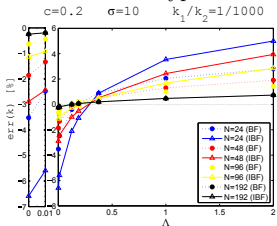
Porous flow across porous cylinder $k_1 \ll k_2$

Effect of Λ on accuracy for $\frac{k_1}{k_2} = \frac{1}{1000}$

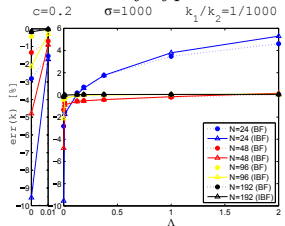
"Stokes-type flow"



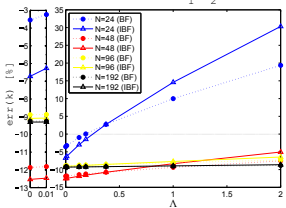
"Brinkman-type flow"



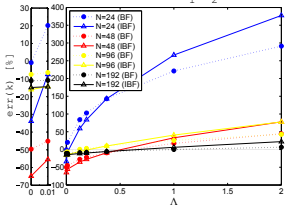
"Darcy-type flow"



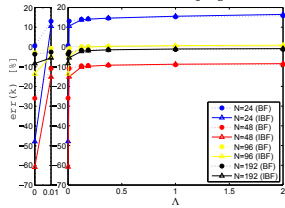
c=0.7 $\sigma=1$ $k_1/k_2=1/1000$



c=0.7 $\sigma=10$ $k_1/k_2=1/1000$

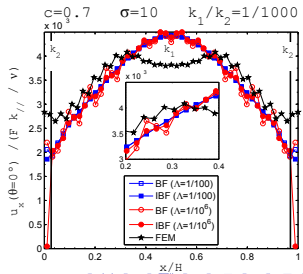
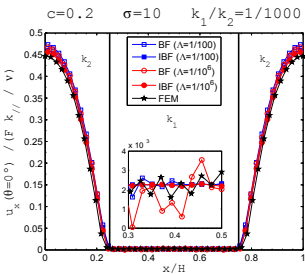
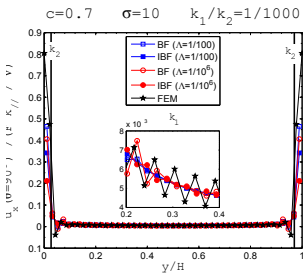
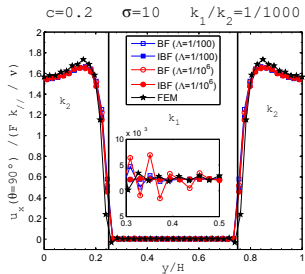


c=0.7 $\sigma=1000$ $k_1/k_2=1/1000$



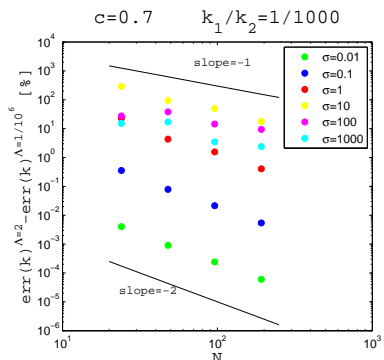
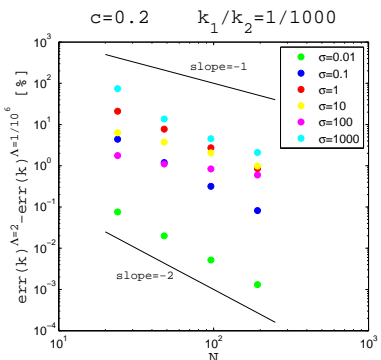
Porous flow across porous cylinder $k_1 \ll k_2$

Effect of IBF on $u_x(y)$ and $u_x(x)$ for $\frac{k_1}{k_2} = \frac{1}{1000}$



Porous flow across porous cylinder $k_1 \ll k_2$

Effect of lattice resolution on accuracy for $\frac{k_1}{k_2} = \frac{1}{1000}$



$\forall \sigma$ spatial convergence rate between 1st- and 2nd-order

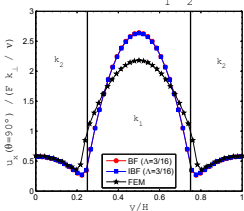
(Data shown for BF model)

Porous flow across porous cylinder $k_1 \gg k_2$

$u_x(y)$ at vertical ($\theta = 90^\circ$) midplane for $\frac{k_1}{k_2} = 1000$ and $c = 0.2$

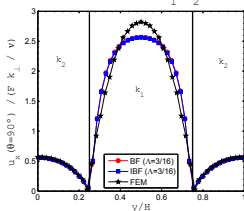
“Stokes-type flow”

$$c=0.2 \quad \sigma=1 \quad k_1/k_2=1000$$



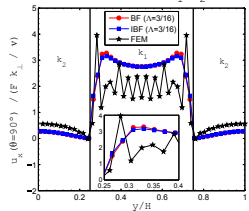
“Brinkman-type flow”

$$c=0.2 \quad \sigma=10 \quad k_1/k_2=1000$$



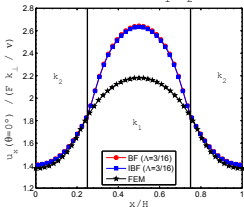
“Darcy-type flow”

$$c=0.2 \quad \sigma=1000 \quad k_1/k_2=1000$$

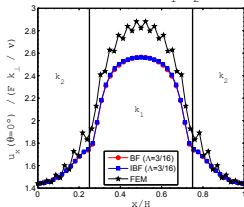


$u_x(x)$ at horizontal ($\theta = 0^\circ$) midplane for $\frac{k_1}{k_2} = 1000$ and $c = 0.2$

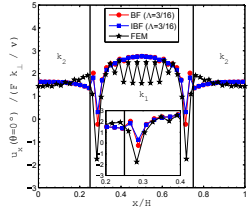
$$c=0.2 \quad \sigma=1 \quad k_1/k_2=1000$$



$$c=0.2 \quad \sigma=10 \quad k_1/k_2=1000$$



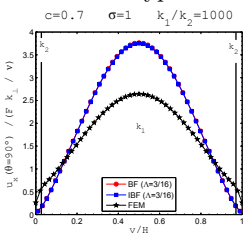
$$c=0.2 \quad \sigma=1000 \quad k_1/k_2=1000$$



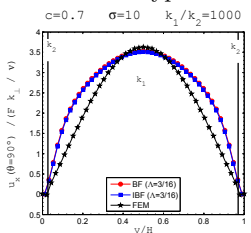
Porous flow across porous cylinder $k_1 \gg k_2$

$u_x(y)$ at vertical ($\theta = 90^\circ$) midplane for $\frac{k_1}{k_2} = 1000$ and $c = 0.7$

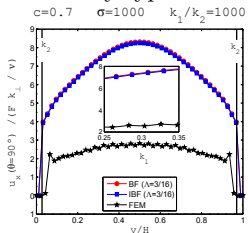
“Stokes-type flow”



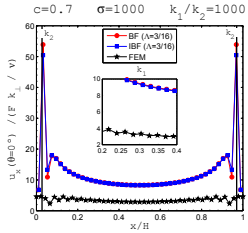
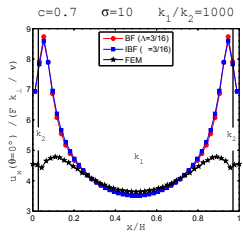
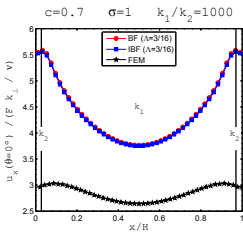
“Brinkman-type flow”



“Darcy-type flow”

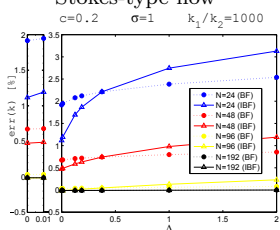


$u_x(x)$ at horizontal ($\theta = 0^\circ$) midplane for $\frac{k_1}{k_2} = 1000$ and $c = 0.7$

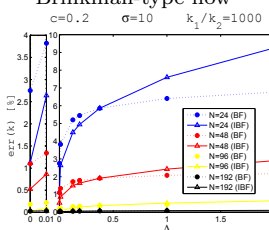


Porous flow across porous cylinder $k_1 \gg k_2$ Effect of Λ on accuracy for $\frac{k_1}{k_2} = 1000$

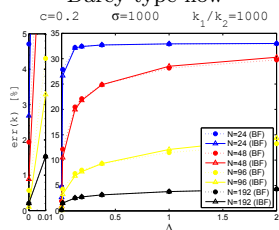
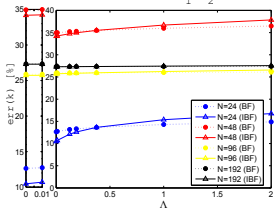
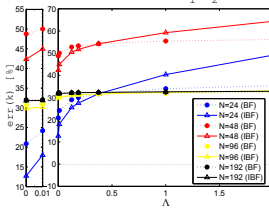
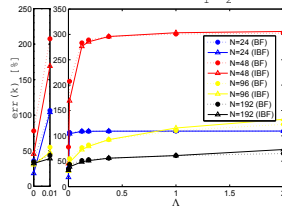
“Stokes-type flow”

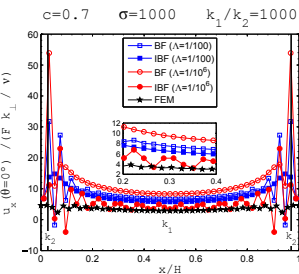
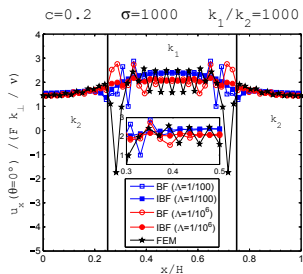
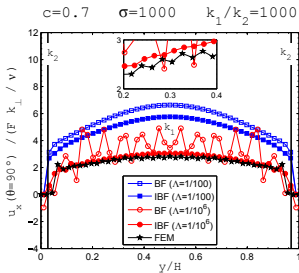
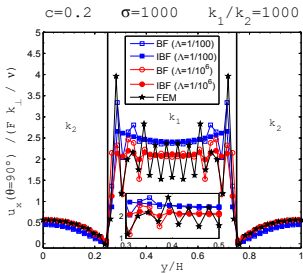


“Brinkman-type flow”



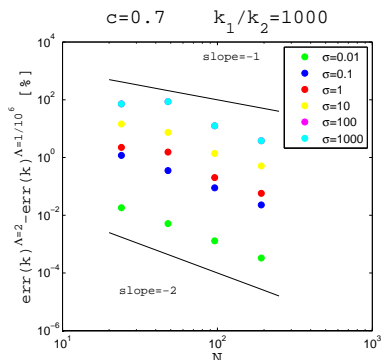
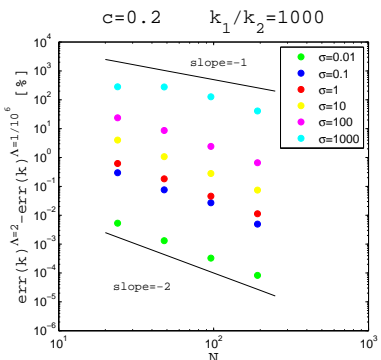
“Darcy-type flow”

 $c=0.7 \quad \sigma=1 \quad k_1/k_2=1000$  $c=0.7 \quad \sigma=10 \quad k_1/k_2=1000$  $c=0.7 \quad \sigma=1000 \quad k_1/k_2=1000$ 

Porous flow across porous cylinder $k_1 \gg k_2$ Effect of IBF on $u_x(y)$ and $u_x(x)$ for $\frac{k_1}{k_2} = 1000$ 

Porous flow across porous cylinder $k_1 \gg k_2$

Effect of lattice resolution on accuracy for $\frac{k_1}{k_2} = 1000$



$\forall \sigma$ spatial convergence rate between 1st- and 2nd-order

(Data shown for BF model)

Conclusions

Biporous medium: $k_1 \ll k_2$

- Solutions behave, approximately, as case of Brinkman flow around solid cylinder.
- However, with interface playing the role of boundary we recover larger errors (particularly in Brinkman regime).
- TRT velocity solutions are *over-estimated*, except for small Λ
- Small Λ values lead to wiggles velocity solution profiles. They are partially corrected by **IBF**
- Dependency on **lattice resolution** indicates spatial convergence rate between 1st – and 2nd–order

Biporous medium: $k_1 \gg k_2$

- TRT velocity solutions are *significantly over-estimated* in Darcy regime. Solution requires use of small Λ
- However, small Λ values produce *strong* wiggles in velocity profiles. They are successfully corrected by **IBF**
- Dependency on **lattice resolution** indicates spatial convergence rate between 1st – and 2nd–order